Parameter study of sound energy distribution in cuboid extra-large spaces

Chao Wang[1], Hui Ma[1], Jian Kang[1,2] (✉)

1. *School of Architecture, Tianjin University, Tianjin 300072, China*

2. *UCL Institute for Environmental Design and Engineering, The Bartlett, University College London (UCL), Central House, 14 Upper Woburn Place, London WC1H 0NN, UK*

Abstract

The aim of this paper is to explore the sound energy distribution in cuboid extra-large spaces. The surface absorption and height are studied as the parameters using the image method. Air absorption is also discussed in this paper. The results show that the difficulty of reducing the noise increases with the increasing volume in extra-large spaces. Even if the ratio between the equivalent absorption area and the total surface is kept constant, the efficiency of noise reduction decreases by approximately 21% in this study. The absorption areas on the floor and the walls have a better performance on noise reduction than that on the ceiling. When the initial height of an extra-large space with general ratio of three dimensions is continuously halved, the variation in the noise level is close to a fixed value, and when the initial height continuously doubled, the noise level decreased approximately exponentially. The predicted difference between with and without consideration of air absorption increases linearly with the source-receiver distance.

1 Introduction

"Diffuse" is an important assumption for many acoustic calculations in general spaces, such as classrooms or auditoriums. However, more and more buildings with extra-large spaces inside have been built worldwide and the sound field in those extra-large spaces will theoretically become more non-diffuse, resulting in uneven energy distribution and non-linear energy decay (Hodgson 1996).

The sound energy distribution in a room is significant for the prediction of speech intelligibility and noise control. In general spaces, based on the assumption of diffuse sound field, speech intelligibility can be predicted by the noise-to-signal ratio (Kryter 1962). Noise reduction due to the addition of the surface absorption can also be evaluated based on two conditions (before and after the treatment using sound absorbing materials) of the total absorption area (Egan 1988). However, sound fields in extra-large spaces are non-diffuse and differ from those in general spaces (Lewers and Anderson 1984; Wang et al. 2018). The sound energy distribution in extra-large spaces cannot be determined directly by the diffuse sound field theory.

A direct way to determine the energy distribution is via the theoretical approach, and several models have been proposed. Barron and Lee (1988) proposed a model that divided the total sound energy into three parts. This model has been discussed continuously (Aretz and Orlowski 2009; Barron 2013; Beranek 2016). In large churches all over the world, measurements have been conducted and several models have been proposed (Anderson and Bratos-Anderson 2000; Cirillo and Martellotta 2003, 2005; Girón et al. 2017). However, all of the models were based on the assumption of diffuse sound field to varying degrees; thus, geometric information such as the shape or sound absorption distribution was not considered in the predicted results.

A parameter study is a direct way to determine the effect of a single variable in room geometry and has been used to explore the sound energy distribution in many non-diffuse sound fields such as long and flat spaces (Hodgson 1994; Kang 1996b; Kuttruff 2009). In long spaces, parameter studies showed that both even and uneven surface absorptions had important effects on sound energy attenuation along the

E-mail: j.kang@ucl.ac.uk

length of the space (Kang 1996a; Picaut et al. 1999). Regarding diffusion, previous studies (Kang 2000; Visentin et al. 2015) showed that the sound energy with diffuse boundaries decreased more rapidly than that with specularly reflecting boundaries along the length. The height and wide-to-height ratio are also important parameters in long spaces. In the street, previous studies showed that the height of buildings had an obvious influence on the curves of the sound energy attenuation along the length (Kang 2001, 2002). In other types of spaces such as flat spaces and coupled spaces, the effects of acoustic parameters such as the surface absorption coefficient and the diffusion coefficient have also been explored using the image method (Galaitsis and Patterson 1976; Hodgson 1988), ray-tracing method (Hodgson 1990; Hou et al. 2017), energy balance method (Anderson et al. 1997), or other approaches (Bistafa and Bradley 2000; Cai et al. 2019; Summers et al. 2004; Xiang et al. 2005, 2011). The results of these parameter studies can give designers and acoustic consultants an intuitive guide at an early design stage. However, a parameter study focusing on the sound energy distribution in extra-large spaces has not been conducted systematically. This becomes increasingly important as more extra-large spaces, which accommodate a large amount of people, are constructed.

Adding surface absorption material is a direct way to reduce the noise level. For this purpose, the noise reduction of reverberant energy due to the addition of surface absorption is generally evaluated with the following equation (Egan 1988):

$$\Delta SPL = 10\log_{10}\frac{A_2}{A_1} \tag{1}$$

where ΔSPL is the reduction of reverberant energy (dB), A_1 is the total room absorption before treatment (m²), and A_2 is the total room absorption after treatment (m²). This equation means that the reverberant noise level will decrease by a fixed value when the surface absorption area is doubled, which is an obvious exponential relation. However, in an extra-large space, which is obviously non-diffuse, it is a question of whether reducing noise using surface absorption still follows the rule of diffuse theory.

Therefore, the aim of this paper is to explore the sound energy distribution in cuboid extra-large spaces with different volumes and surface absorption values. The effect of the absorption distribution, height, and air absorption was also studied using the image method.

2   Methodology

In this paper, the acoustic variables were studied individually, and computer simulations were used to avoid the influence

of other factors. An image method introduced by Gibbs and Jones (1972) is used to investigate sound distribution in extra-large spaces. Different absorptions, absorption distributions, room heights, and air absorptions are compared in different models. More details are provided in the following subsections.

2.1   Simulated models

In general, a cuboid space is always described by three dimensions: length, width, and height. Except for some factories and cathedrals, the height of large spaces rarely exceeds 50 m, especially spaces that accommodate a large number of people. The width is usually within 100 m due to the structural span limitation. As the most unrestricted dimension, the length is usually extended to varying degrees to obtain the required space. For example, the three dimensions of three typical extra-large spaces in China are 285 m × 85 m × 35 m (Changchun Station), 220 m × 87 m × 34 m (Shenyang Station), and 152 m × 62 m × 21 m (Dianchi Convention and Exhibition Centre, Kunming). Thus, it is reasonable in this study to consider, for simplicity, a virtual size of 300 m × 100 m × 50 m as the hypothetical maximum size (in this situation, length:width:height is 6:2:1). Thus, a series of models with a constant ratio of the three dimensions of 6:2:1 (length:width:height) are studied in this paper, and a series of cubic virtual models with the same width are also investigated using the same method for comparison. The two types of shapes are shown in Fig. 1 and are called Type I and Type II respectively. The cases of 150 m for width in both two types are also considered to explore some extreme situations might occur in the future. The three dimensions of all of the models are shown in Table 1 except for additional explanation.

Because crowd noise is usually the major noise source in an extra-large space, the source point was arranged in the centre of the floor at a height of 1.5 m, and the receiver points were arranged at a height of 1.2 m. To evaluate the sound level in each space, 99 points (10 × 10 minus the 1
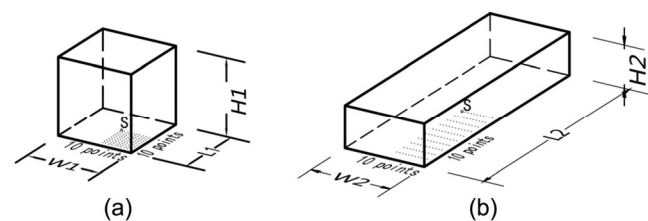
Fig. 1 Two types of virtual initial models ((a) Type I; (b) Type II; *L*: length, *W*: width, *H*: height). The ratio of the three dimensions of Type I (*L*1:*W*1:*H*1) is 1:1:1; the ratio of the three dimensions of Type II (*L*2:*W*2:*H*2) is 6:2:1. S is the sound source, and the small points are the receivers

Table 1 Three dimensions of all of the models used in the studies of absorption distribution (the results are listed in Section 3.1 and Section 3.2)

Model	Type I				Type II			
	L	W	H	Volume (m³)	L	W	H	Volume (m³)
A	20	20	20	8000	40	20	10	8000
B	40	40	40	64,000	120	40	20	96,000
C	60	60	60	216,000	180	60	30	324,000
D	80	80	80	512,000	240	80	40	768,000
E	100	100	100	1,000,000	300	100	50	1,500,000
F	150	150	150	3,375,000	450	150	75	5,062,500

source point) were arranged evenly in a quarter of the floor because of the symmetry, which is shown in Fig. 1. Then, the arithmetic mean value of 99 points was calculated to evaluate the sound level in the space.

2.2 Absorption distribution

A series of virtual cuboid models of two types were simulated to obtain the spatial distribution of the sound energy in cuboid extra-large spaces with different volume and surface absorption. Regarding the size of the existing large spaces, their widths varied from 20 to 150 m (namely the situations of 20, 40, 60, 80, 100, and 150 m are considered). For comparison, different surface absorptions were also applied to each model which has an initial absorption.

In general, building surfaces can be divided into three parts: ceiling, walls, and floor. For different acoustic purposes, varying amounts of absorption material are arranged on them. Then the level of noise reduction, which is represented by the difference of the average sound pressure level (SPL), will be compared in the spaces with different volumes for two types. To evaluate the effect of the surface absorption distribution, a series of spaces with a fixed initial surface absorption coefficient and different volumes were modelled (the initial absorption coefficient of each surface was 0.1).

Then, a series of given absorption areas were added to the ceiling, walls, and floor for comparison. The amount of the added absorption area was calculated by multiplying the floor area by the absorption coefficients (situations from 0 to 0.6) in each space of two types. The simulated models are listed in Table 2, and the method of adding the absorbing material is shown in Fig. 2. Because there are four walls in a space, the amount of the absorption area added on each wall was equal to a quarter of that on the other two positions.

2.3 Height selection

Buildings are designed with different heights to meet varying requirements. In addition to the models described in the Section 2.1, to evaluate the influence of height on the energy distribution, five different height coefficients β (0.25, 0.5, 1, 2, and 4) were used in a series of initial spaces, while the other two dimensions remained unchanged. Then nine different height coefficients (0.0625, 0.125, 0.25, 0.5, 1, 2, 4, 8 and 16) were adopted for further analysis. The final height in a model is calculated as

$$H_{\mathrm{m}} = \beta \cdot H \qquad (2)$$

where, H is the initial height of the initial model. All of the final heights of the simulated models are listed in Table 3. The sound absorption coefficients of 0.1 and 0.5 were uniformly applied to all of the models with different heights to explore the effects of height under different sound absorption coefficients.

Different heights create different spatial shapes, some of which are real, and others are still virtual until now. In Type I models, height coefficients of 0.25 and 0.5 mean that the space is flat. These spaces can be found in general open offices and factories. Height coefficients of 2 and 4 mean that the space is tall. These spaces can be discovered in some atriums and cathedrals. In Type II, spaces with different height coefficients mean different flat or near-flat spaces, which are very common in practise.

Table 2 Final absorption of all the three positions used to investigate the effect of absorption distribution. α_0, which is discussed in the case of two values of 0.1 and 0.5, is the initial absorption coefficient of all of the models. For a model, S_f is the area of the floor. S_{w1}, S_{w2}, S_{w3}, and S_{w4} are the area of the four walls. S_c is the area of the ceiling. $\alpha \times S_f$ or $1/4\,\alpha \times S_f$ is the added absorption area

	Adding position	Final absorption					
		Floor	Wall 1	Wall 2	Wall 3	Wall 4	Ceiling
Even distribution (results in Section 3.1)	Floor, walls, and ceiling	$(\alpha_0 + \alpha) \times S_f$	$\alpha_0 \times S_{w1} + \frac{1}{4}\alpha \times S_f$	$\alpha_0 \times S_{w2} + \frac{1}{4}\alpha \times S_f$	$\alpha_0 \times S_{w3} + \frac{1}{4}\alpha \times S_f$	$\alpha_0 \times S_{w4} + \frac{1}{4}\alpha \times S_f$	$\alpha_0 \times S_c + \alpha \times S_f$
Uneven distribution (results in Section 3.2)	Floor	$(\alpha_0 + \alpha) \times S_f$	$\alpha_0 \times S_{w1}$	$\alpha_0 \times S_{w2}$	$\alpha_0 \times S_{w3}$	$\alpha_0 \times S_{w4}$	$\alpha_0 \times S_c$
	Wall	$\alpha_0 \times S_f$	$\alpha_0 \times S_{w1} + \frac{1}{4}\alpha \times S_f$	$\alpha_0 \times S_{w2} + \frac{1}{4}\alpha \times S_f$	$\alpha_0 \times S_{w3} + \frac{1}{4}\alpha \times S_f$	$\alpha_0 \times S_{w4} + \frac{1}{4}\alpha \times S_f$	$\alpha_0 \times S_c$
	Ceiling	$\alpha_0 \times S_f$	$\alpha_0 \times S_{w1}$	$\alpha_0 \times S_{w2}$	$\alpha_0 \times S_{w3}$	$\alpha_0 \times S_{w4}$	$\alpha_0 \times S_c + \alpha \times S_f$
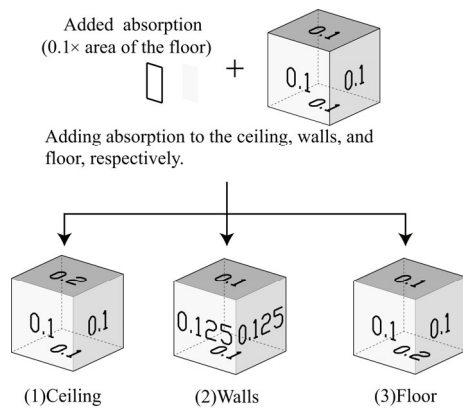
Fig. 2 The Surface absorption (equal to 0.1 × area of floor) added to the different positions in a Type I space. The initial surface absorption is also 0.1 (There is also a case where the initial surface absorption coefficient is 0.5.). The final absorption is represented by the absorption coefficient shown on the surface

Table 3 Three heights of all the models used in the studies of the effect of height (the results are listed in Section 3.3)

Initial model	Height coefficient								
	0.0625	0.125	0.25	0.5	1	2	4	8	16
Type I A	*	2.5	5	10	20	40	80	160	320
B	2.5	5	10	20	40	80	160	320	640
C	3.75	7.5	15	30	60	120	240	480	960
D	5	10	20	40	80	160	320	640	1280
E	6.25	12.5	25	50	100	200	400	800	1600
F	9.375	18.75	37.5	75	150	300	600	1200	2400
Type II A	*	*	2.5	5	10	20	40	80	160
B	*	2.5	5	10	20	40	80	160	320
C	1.875	3.75	7.5	15	30	60	120	240	480
D	2.5	5	10	20	40	80	160	320	640
E	3.125	6.25	12.5	25	50	100	200	400	800
F	4.6875	9.375	18.75	37.5	75	150	300	600	1200

* means that the height is too low, so that the source or receiver is out of model.

The receiver points are distributed evenly to explore the average difference in the sound pressure level with changes in the height. The information of the receiver is the same as in the Section 2.1.

2.4   Air absorption

As the mean free path increases with increasing volume in a diffuse field, the sound will spread farther; thus, air absorption in the space will increase as well. Although the sound field in an extra-large space is obviously non-diffuse, the air absorption might become more important with an increase in volume. In addition to the aforementioned studies, the effect of air absorption will also be assessed by calculating the ratio of the sound energy absorbed by air to the total absorbed energy at different receivers using the image method. As an additional part, only six cubic models were studied. The width of the simulated models are 10 m, 30 m, 50 m, 100 m, 300 m, and 500 m.

2.5   Simulation setting

An image method introduced by Gibbs and Jones (1972) was used in this study because its algorithm is easy to implement and the result of the reflection sequence is accurate (Dance and Shield 1997; Lehmann and Johansson 2008). A theoretical model based on the principle of this method was used to explore energy intensity in the 1950s (Bolt et al. 1950; Doak 1959). In addition, unlike many other algorithms, the computational efficiency of this algorithm is independent of the volume, which provides more advantages in extra-large spaces. However, wave effects such as the edge effect and low-frequency resonance, which are important in small rooms, were not under consideration. Diffusion was also not considered, for simplicity.

In all of the calculations, the background noise level was set to 10 dB, and the air absorption coefficient was set to 0.00986 dB/m (2000 Hz, 20 °C, and 50% relative humidity, based on ISO9613-1:1993). The cut-off condition was set to -100 dB below the background noise to collect as much sound reflection as possible. This method and settings were achieved using the Python language in Anaconda software (Python 3.6.5 and Anaconda 3.5.1) for better customisation and usability.

3   Results and discussion

This parameter study focusing on the sound energy distribution in cuboid extra-large spaces has been carried out in the following three aspects in Type I and Type II models: (1) the effect of increasing absorption in the case of even absorption distribution; (2) The difference in the effect of absorption on different positions (floor, walls and ceiling) in the case of uneven absorption distribution; and (3) the effect of variable height with fixed length and width. The effect of air absorption in cubic extra-large spaces is also studied.

3.1   Even surface absorption

In this section, the absorption of all of the surfaces is even, and the results are shown in Figs. 3(a) to (f). Figure 3 represents, for six different models in Table 1 and for the varying absorption coefficients, the sound pressure level as a function of the source-receiver distance. The curves represent the 99 receiver points as described in Section 2.1. This indicates that the sound field in all of the spaces are
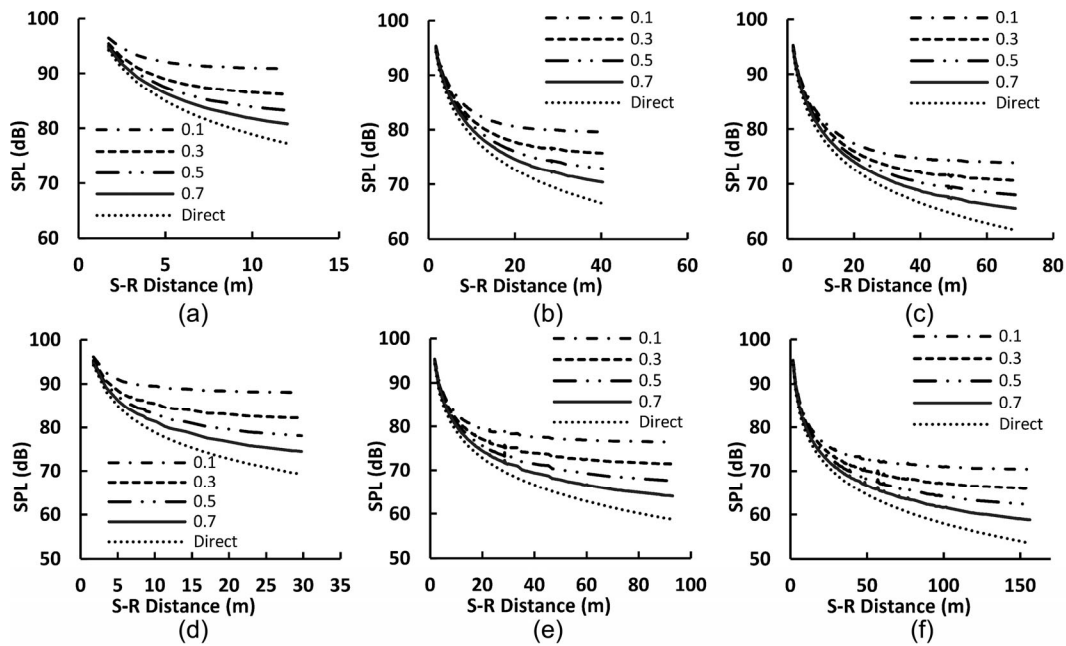
Fig. 3 The sound pressure level as a function of the source-receiver distance when different surface absorption is added to all the six surfaces evenly. In each figure, the different curves mean different added absorption as described in Fig. 2 (Type I: (a) is in a space 20 m × 20 m × 20 m, (b) is in a space 60 m × 60 m × 60 m, (c) is in a space 100 m × 100 m × 100 m. Type II: (d) is in a space 20 m × 60 m × 10 m, (e) is in a space 60 m × 180 m × 30 m, (f) is in a space 100 m × 300 m × 50 m)

non-diffuse. Most of the curves in six figures decrease exponentially, which means that the energy decreases rapidly in near-source area and slowly far from the source.

In Fig. 3, both the spatial volume and surface absorption influence the pattern of the decreasing curves. With an increase in the volume and surface absorption, the curve of the total energy gradually approaches the curve of the direct energy. However, when the volume becomes extremely large and the surface absorption becomes very high (such as curve 0.7 in Figs. 3(c) or 3(f)), the total energy curve far from the source area is still several decibels higher than the direct energy curve. This indicates that reverberant energy is difficult

to be absorbed completely and still occupies a large proportion of the total sound energy, which cannot be neglected. This is why it is very difficult to manage high crowd noise in an extra-large space. It is difficult to completely absorb the crowd noise, as it spreads far away and affects the entire sound field. When there are many sound sources, such as a large number of people, in an extra-large space, the accumulation of the crowd noise energy will cause a high level of background noise.

The average sound pressure level with an increase in the surface absorption in two types of spaces is shown in Fig. 4. Based on the diffuse sound field theory and Eq. (1),
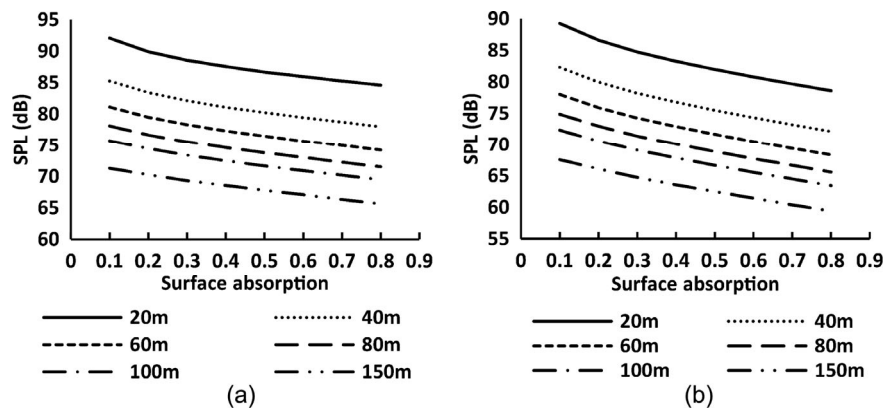
Fig. 4 The average sound pressure level with an increase in the surface absorption in two types of spaces. The average sound pressure level is calculated by taking the arithmetic average of the results of 99 receivers described in Section 2.1. The curves represent the width of the space, and all the three dimensions are listed in Table 1 ((a) in a Type I space, (b) in a Type II space)

the reverberant sound pressure level is a constant in a space and decreases exponentially with an increase in the surface absorption, and the direct sound pressure level decreases exponentially along the source-receiver distance. However, when these two parts of noise energy are added, all of the curves in the two types of spaces show a linear trend in Fig. 4, especially when the volume increases. This result shows that both the direct and reverberant energies occupy a considerable proportion of the total energy.

However, a slight exponential trend still appears in a space with small volume and low surface absorption, including the top three curves for both Type I and Type II (which means the width of the space is less than or equal to 60 m). This indicates that when the surface absorption is low and the volume is not very large, the addition of the same surface absorption area can reduce more noise. However, when a space becomes larger or the surface absorption of the space is not very low (larger than 0.2 in the simulated cases in this study), the addition of surface absorption reduces the average total noise level by a fixed value, which is further studied below using linear regression analysis below.

The results of the linear regression analysis of all of the curves in Figs. 4(a) to (b) are listed in Table 4. All of the coefficients of determination are higher than 0.95, which shows a strong linearity of the curves. The results demonstrate that with an increase in volume, the slopes of the curves become flatter, from −10.02 to −7.95 for Type I and from −14.6 to −11.49 for Type II, both decreasing approximately about 21%. This means that reducing the noise in larger space becomes more difficult even when the same proportion of surface absorption is used. From another perspective, this also explains why the crowd noise in extra-large space is so difficult to reduce.

There are some differences between Type I and Type II in terms of noise reduction using sound absorbing materials. In a space of Type I, with the sound absorption coefficient varying from 0.1 to 0.8, the average noise level decreases by different values. The reduced values vary from 7.45 dB in the cubic space 20 m × 20 m × 20 m to 5.67 dB in the cubic space 150 m × 150 m × 150 m. In a space of Type II, the

reduced average noise levels vary from 10.67 dB (in the space 20 m × 60 m × 10 m) to 8.17 dB (in the space 150 m × 450 m × 75 m). This indicates that the noise in the Type I space is easier to reduce than that in Type II space.
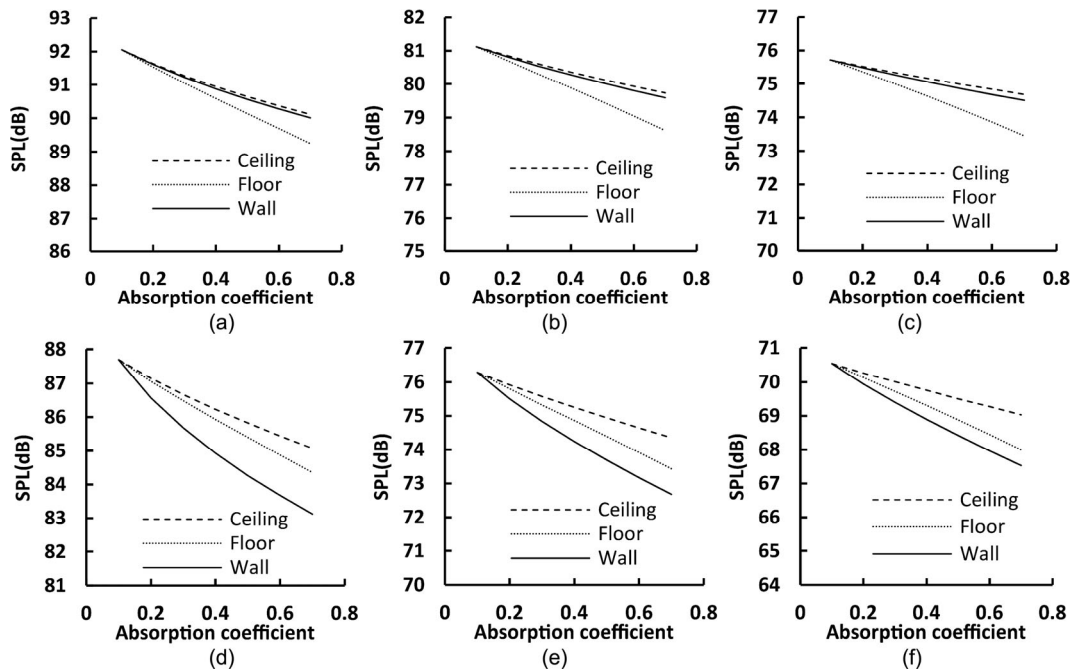
3.2 Effect of absorption distribution

The results in Figs. 5(a) to (f) show that the sound absorption in varying positions can reduce the noise levels differently. The linear regression analysis results of all of the curves in Fig. 5 are listed in Table 5. For Type I, the absorption area on the floor has better performance than areas on the other two positions. The absorption area on the wall is just slightly better than that on the ceiling. With an increase in volume, the difference between the curves of the floor and the other two positions increases, although the curves of all three positions become flatter. This indicates that with an increase in volume, although the performance of absorption on all three positions decreases, the floor shows more of an advantage than the other positions.

In Type II, the absorption area on the wall has the best performance, and the floor is a better position than the ceiling, as shown in Fig. 5. It is interesting that with an increase in volume, the difference between the curves of the wall and the other two positions decreases, although all of the curves become flatter. This means that the performance of absorption in all three positions decreases, and their difference in noise reduction becomes smaller. When the volume becomes larger (from 12,000 m^3 to 1,500,000 m^3), the curve of the floor gradually turns from close to the ceiling to closer to the wall. This means that the floor is also a good position for noise reduction in Type II extra-large spaces.

Because of the high determination coefficient of the curves, the slope can be used to directly evaluate the noise reduction performance. As in Section 3.1, with an increase in the amount of sound absorption, the average noise level in the same space reduces linearly with a very high coefficient of determination ($R^2 = 0.992 - 1$), as shown in Table 5. Noise reduction in the space with uneven surface absorption also shows more difficulty with an increase in volume. For the floor in the Type I spaces, when the volume varies from 8,000 m^3 to 1,000,000 m^3, this slope is from −4.63 to −3.76. For the wall in the Type II spaces, when the volume varies from 12,000 m^3 to 1,500,000 m^3, this slope is from −7.48 to −4.99. This also indicates a limitation to the method of adding surface absorption material to reduce the noise. This limitation becomes more obvious with increasing volume.

3.3 Effect of height

To evaluate the influence of height on the energy distribution,

Table 4 Linear regression analysis results of the decreasing curves related to the decrease in the average total noise level to the increase in the surface absorption in two types of spaces

		Size (m)					
		20	40	60	80	100	150
Type I	Slope	−10.02	−9.93	−9.53	−9.11	−8.73	−7.95
	R^2	0.954	0.971	0.98	0.986	0.989	0.995
Type II	Slope	−14.6	−14.06	−13.46	−12.93	−12.46	−11.49
	R^2	0.974	0.982	0.986	0.99	0.992	0.995

Fig. 5 The average sound pressure level in a space after a series of surface absorptions were added at different positions. The average sound pressure level is calculated by taking the arithmetic average of the results of 99 receivers described in Section 2.1 (The *x*-axis represents the final surface absorption coefficient of the floor after the addition of surface absorption, as listed in Table 2. Type I: (a) is in a space 20 m × 20 m × 20 m, (b) is in a space 60 m × 60 m × 60 m, and (c) is in a space 100 m × 100 m × 100 m. Type II: (d) is in a space 20 m × 60 m × 10 m, (e) is in a space 60 m × 180 m × 30 m, and (f) is in a space 100 m × 300 m × 50 m)

Table 5 Linear regression analysis results of the curves related to an average reduction in the sound pressure level to the added absorption area (represented by the absorption coefficient) in different spaces

	Size (m)	20			60			100		
	Position	Floor	Wall	Ceiling	Floor	Wall	Ceiling	Floor	Wall	Ceiling
Type I	Slope	−4.63	−3.37	−3.19	−4.15	−2.53	−2.30	−3.76	−2.01	−1.72
	R^2	0.999	0.992	0.993	1.000	0.996	0.997	1.000	0.998	0.998
Type II	Slope	−5.53	−7.48	−4.33	−4.74	−5.95	−3.20	−4.23	−4.99	−2.51
	R^2	0.999	0.984	0.995	1.000	0.993	0.998	1.000	0.997	0.999

five different height coefficients β (0.25, 0.5, 1, 2, and 4) were used in a series of initial spaces, while the other two dimensions remained unchanged. The sound pressure level as a function of the source-receiver distance in initial spaces after the change in height is shown in Figs. 6(a) to (f) for Type I models and Figs. 7(a) to (f) for Type II models. In the spaces of two types of models, some similar trends are found in the attenuation of the sound pressure level. First, in the space with different heights, the sound energy attenuates differently, and the largest difference always appears in the area farthest from the source. This phenomenon becomes more obvious in larger spaces, which indicates that the sound field in larger space becomes less diffuse. Second, the attenuation curves become more exponential with increasing volume. This is because the reverberant energy is weakened as the volume increases. Another phenomenon

can also be attributed to the weakened reverberant energy: in the same initial space, when the surface absorption coefficient becomes larger, the difference caused by the different heights becomes smaller.

There are some additional differences between the results of the two types. First, the sound pressure level for Type II attenuates more exponentially than that for Type I, especially in the near-source area. This is due to the different shapes of the two types. Second, the sensitivity of the attenuation curve to the height is different in the two types of spaces. The difference between the curves in the Type I spaces are more sensitive to flattening, and the difference between the curves in the Type II spaces are more sensitive to heightening.

To evaluate the sensitivity of the SPL attenuation to the change in height, nine different height coefficients (0.0625,
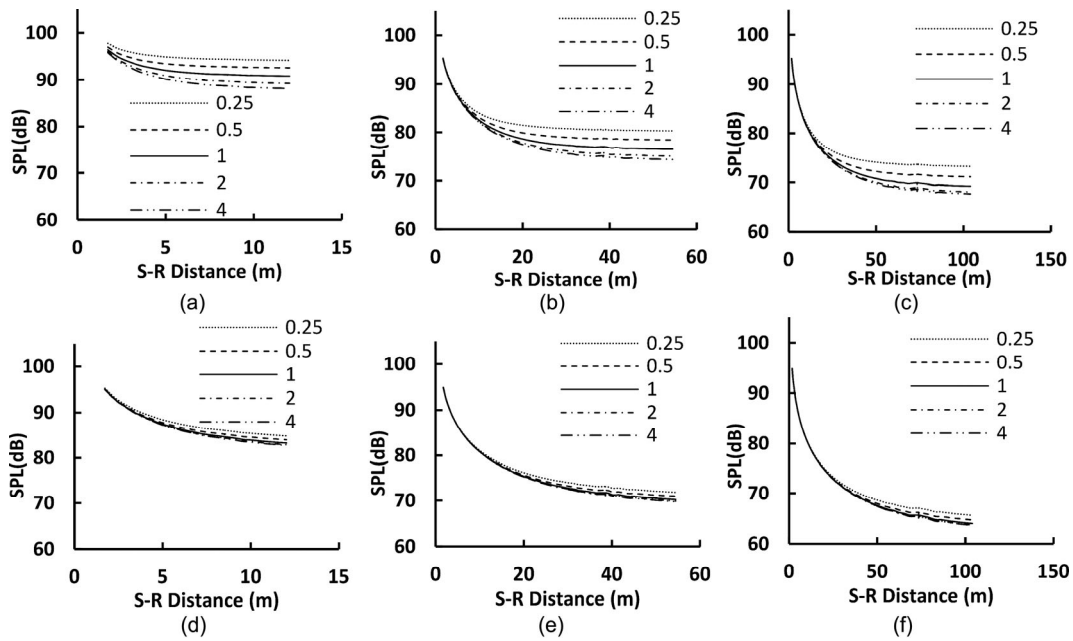
Fig. 6 The sound pressure level as a function of the source-receiver distance in six initial spaces of Type I after the height of the space was changed according to the different height coefficients, as the corresponding part in Table 3. The different curves represent the different height coefficients. For example, the curve named 1 represents the result in the initial model (three dimensions–surface absorption of initial model: (a) 20 m × 20 m × 20 m–0.1, (b) 80 m × 80 m × 80 m–0.1, (c) 150 m × 150 m × 150 m–0.1, (d) 20 m × 20 m × 20 m–0.5, (e) 80 m × 80 m × 80 m–0.5, and (f) 150 m × 150 m × 150 m–0.5)
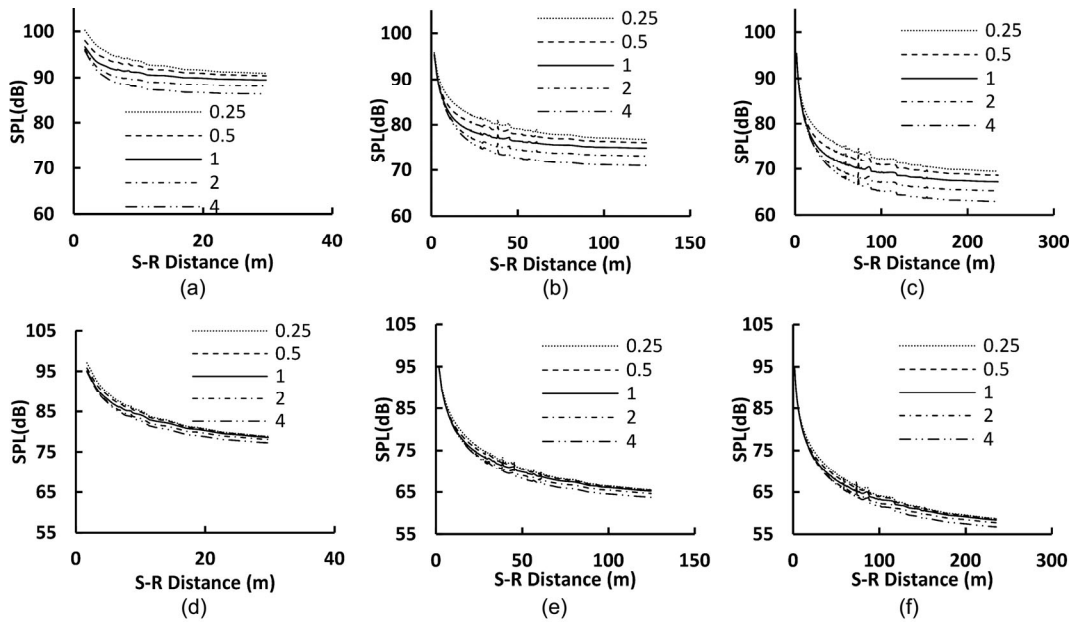
Fig. 7 The sound pressure level as a function of the source-receiver distance in six initial spaces of Type II after the height of the space is changed according to the different height coefficients, as the corresponding part in Table 3. The different curves represent the different height coefficients. For example, the curve named 1 represents the result in the initial model (three dimensions–surface absorption of initial model: (a) 60 m × 20 m × 10 m–0.1, (b) 240 m × 80 m × 40 m–0.1, (c) 900 m × 150 m × 75 m–0.1, (d) 60 m × 20 m × 10 m–0.5, (e) 240 m × 80 m × 40 m m–0.5, and (f) 900 m × 150 m × 75 m–0.5)

0.125, 0.25, 0.5, 1, 2, 4, 8 and 16) were adopted for further analysis. The results are shown in Figs. 8(a) to (f). The results demonstrate that when the initial space is flattened or heightened, the spoon-shaped curves indicate that the

variation in the average noise level has almost similar trends in the two types of space with different volumes. When the initial height of the space is halved each time, which means the space is flattened, the variation in the sound pressure
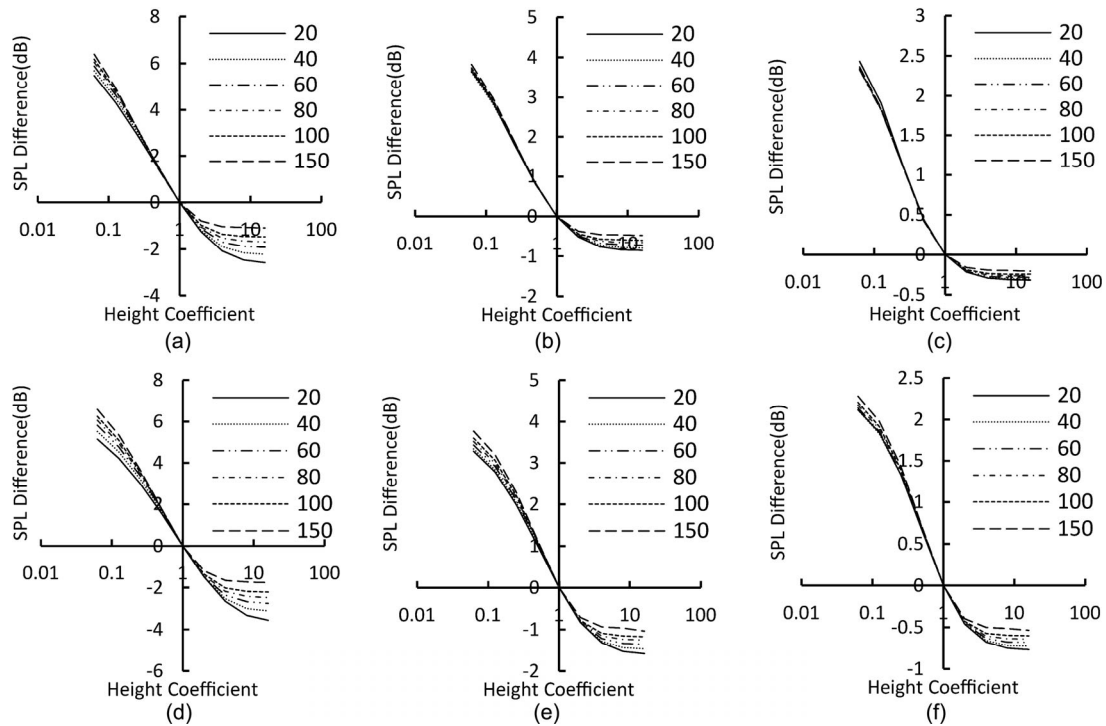
Fig. 8 Difference of average sound pressure level in space with different volumes when height is changed based on height coefficient. The x-axis is logarithmic. The curves represent the width of the initial space, all the three dimensions of which are listed in Table 1. All the heights of simulated models are listed in Table 3 (surface absorption: (a) Type I-0.1, (b) Type I-0.3, (c) Type I-0.5, (d) Type II-0.1, (e) Type II-0.3, (f) Type II-0.5)

level is close to a fixed value, which will be further studied using logarithmic regression analysis. When the initial height of the space is doubled each time, which means the space is heightened, the variation in the sound pressure level shows an approximately exponential decrease to varying degrees. The results of logarithmic regression analysis through the points above and under the x-axis are listed in Table 6.

When the height of the space changes little (the height coefficient is approximately 1), the curves almost coincide in the six figures. This means that the same proportional change in height can cause almost the same variation in the average noise level in a space with the same surface absorption. Even in a space with a large volume, this phenomenon still exists. With an increase in the surface absorption as in Fig. 8, the curves increasingly converge and become flatter with an

increase in the height coefficient. The slope of the logarithmic regression of all of the curves changes from -1.5 to -0.49 for Type I and from -1.7 to -0.58 for Type II.

3.4 Effect of air absorption

The ratio of the energy absorbed by air to the total absorbed energy at all of the receiver points are collected to evaluate the spatial variation using the arithmetic mean method in each space, which is shown in Fig. 9. The results show that air absorption is more important when the volume becomes larger. Little spatial variation exists in a space with a normal volume, but a difference appears when the volume is very large. When the volume is larger than 127,000,000 m³ (with a side length of 300 m), the ratio rises rapidly with an increase

Table 6 Logarithmic regression analysis of the curves of the differences in the average noise level related to the height coefficient. The curves are divided into two groups (≥ 1 and ≤ 1)

	Surface absorption	0.1		0.3		0.5	
	Height factor	≤ 1	≥ 1	≤ 1	≥ 1	≤ 1	≥ 1
Type I	Slope (ln$x$)	-2.17	-0.63	-1.37	-0.23	-0.88	-0.09
	R^2	0.992	0.656	0.997	0.666	0.993	0.655
Type II	Slope (ln$x$)	-2.15	-0.93	-1.28	-0.45	-0.8	-0.22
	R^2	0.974	0.74	0.976	0.75	0.75	0.718
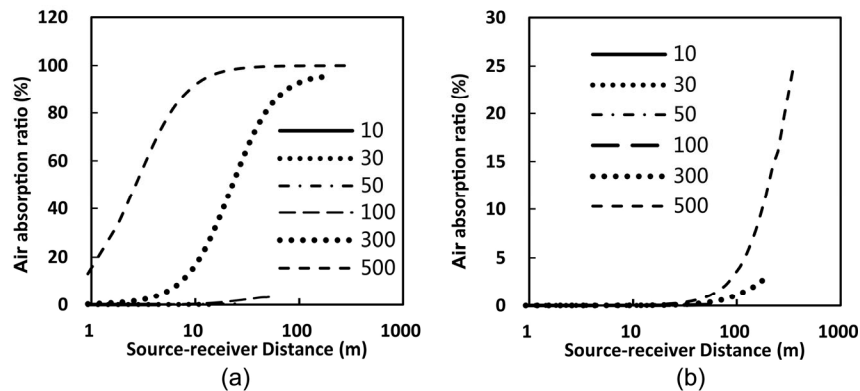
Fig. 9 Ratio of energy absorbed by air to total absorbed energy as a function of source-receiver distance in different spaces: (a) is in space where surface absorption is 0.3 and distributed evenly; (b) is in space where surface absorption is 0.7 and distributed evenly. The curves represent the width of the simulated cubic models
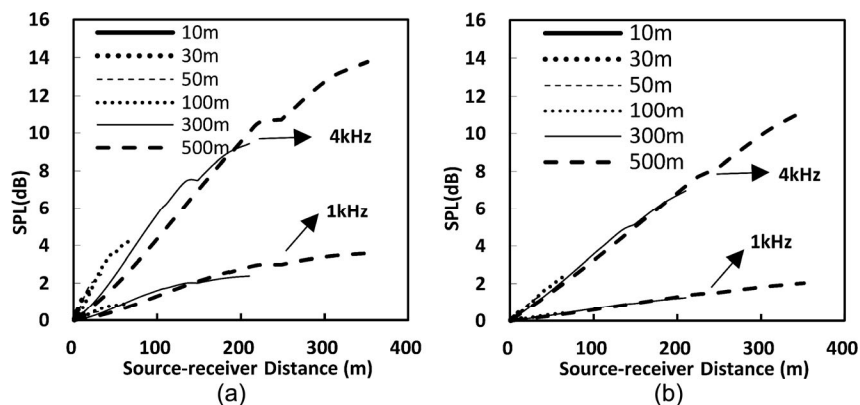
in the source-receiver distance.

Air absorption below 2 kHz is usually not considered in general spaces. However, with an increase in volume, a difference appears. As shown in Figs. 10(a) and (b), the average predicted difference in sound pressure levels with and without air absorption is affected by the source-receiver distance, volume of space, the performance of surface absorption and the considered frequency. First, it increases linearly with the source-receiver distance, and this linear relationship is more obvious with an increase in the surface absorption. This linearity is probably due to the direct sound and early reflections, which carry most of the energy in extra-large spaces. Second, the importance of air absorption increases with increasing volume and decreases as the performance of surface absorption. Based on Fig. 10, if 0.5 dB at 1 kHz is considered the limitation of the prediction difference due to the consideration of air absorption, the following conclusions can be obtained. When the average surface absorption coefficient is 0.3, the minimum volume of a space in which the air absorption should be considered

is 125,000 m³ (that is, the side length is 50 m), and when the average surface absorption coefficient is 0.7, the minimum volume is 27,000 m³ (that is, the side length is 30 m). Finally, higher frequency will bring more air absorption and result in a greater prediction difference. In a space in which the average absorption coefficient is 0.3, the slopes of the curves in Fig. 10 at 1 kHz and 4 kHz are −0.01 dB/m and −0.04 dB/m, respectively.

4   Conclusions

A parameter study was conducted to explore the sound energy distribution in cuboid extra-large spaces. A series of simulations were carried out in two types of hypothetical spaces, leading to several conclusions. First, even when a high level of surface absorption is applied to an extra-large space, the reverberant energy still occupies a large proportion in total energy, especially in the area farthest from the source. This indicates the difficulty of managing crowd noise in extra-large spaces. In addition, as the volume increases, it

Fig. 10 Average predicted difference in sound pressure levels with and without air absorption as a function of source-receiver distance in different spaces: (a) is in space where surface absorption is 0.3 and distributed evenly; (b) is in space where surface absorption is 0.7 and distributed evenly. The curves represent the width of the simulated cubic models

becomes more difficult to reduce the crowd noise using the same proportion of surface absorption.

Second, simulations in two types of spaces with uneven surface absorptions show that the absorption areas on the floor and the walls have a better performance on noise reduction than that on the ceiling. In the cubic models (Type I), the floor shows the greatest advantage among the three positions. In the practical models (Type II), the wall shows the greatest advantage.

Third, with a change in height, the noise levels in cubic and practical spaces show similar spoon-shaped trends. When the initial height of an extra-large space is halved each time, the variation in the sound pressure level is close to a fixed value. When the initial height of the space is doubled each time, the variation of the sound pressure level shows an approximately exponential decrease.

Finally, the air absorption becomes more important when the volume increases. The prediction difference of whether to consider the air absorption increases linearly with the source-receiver distance. If 0.5 dB is considered as the limitation of the prediction difference at 1 kHz, the minimum volume of a space in which the air absorption should be considered is suggested with different surface absorptions.

Acknowledgements

References

Anderson JS, Bratos-Anderson M (2000). Acoustic coupling effects in St Paul's Cathedral, London. *Journal of Sound and Vibration*, 236: 209–225.

Anderson JS, Bratos-Anderson M, Doany P (1997). The acoustics of a large space with a repetitive pattern of coupled rooms. *Journal of Sound and Vibration*, 208: 313–329.

Aretz M, Orlowski R (2009). Sound strength and reverberation time in small concert halls. *Applied Acoustics*, 70: 1099–1110.

Barron M (2013). Objective assessment of concert hall acoustics using Temporal Energy Analysis. *Applied Acoustics*, 74: 936–944.

Barron M, Lee LJ (1988). Energy relations in concert auditoriums. I. *The Journal of the Acoustical Society of America*, 84: 618–628.

Beranek LL (2016). Concert hall acoustics: Recent findings. *The Journal of the Acoustical Society of America*, 139: 1548–1556.

Bistafa SR, Bradley JS (2000). Predicting reverberation times in a simulated classroom. *The Journal of the Acoustical Society of America*, 108: 1721–1731.

Bolt RH, Doak PE, Westervelt PJ (1950). Pulse statistics analysis of room acoustics. *The Journal of the Acoustical Society of America*, 22: 328–340.

Cai M, Lan Z, Zhang Z, Wang H (2019). Evaluation of road traffic noise exposure based on high-resolution population distribution and grid-level noise data. *Building and Environment*, 147: 211–220.

Cirillo E, Martellotta F (2003). An improved model to predict energy-based acoustic parameters in Apulian-Romanesque churches. *Applied Acoustics*, 64: 1–23.

Cirillo E, Martellotta F (2005). Sound propagation and energy relations in churches. *The Journal of the Acoustical Society of America*, 118: 232–248.

Dance SM, Shield BM (1997). The complete image-source method for the prediction of sound distribution in non-diffuse enclosed spaces. *Journal of Sound and Vibration*, 201: 473–489.

Doak P (1959). Fluctuations of the sound pressure level in rooms when the receiver position is varied. *Acta Acustica united with Acustica*, 9: 1–9.

Egan MD (1988). Architectural Acoustics. New York: McGraw-Hill Custom Publishing.

Galaitsis AG, Patterson WN (1976). Prediction of noise distribution in various enclosures from free-field measurements. *The Journal of the Acoustical Society of America*, 60: 848–856.

Gibbs BM, Jones D (1972). A simple image method for calculating the distribution of sound pressure levels within an enclosure. *Acta Acustica united with Acustica*, 26: 24–32.

Girón S, Álvarez-Morales L, Zamarreño T (2017). Church acoustics: A state-of-the-art review after several decades of research. *Journal of Sound and Vibration*, 411: 378–408.

Hodgson M (1988). On the prediction of sound fields in large empty rooms. *The Journal of the Acoustical Society of America*, 84: 253–261.

Hodgson M (1990). Evidence of diffuse surface reflection in rooms. *The Journal of the Acoustical Society of America*, 88(S1): S185–S185.

Hodgson M (1994). When is diffuse-field theory accurate? *Canadian Acoustics*, 22: 41–42.

Hodgson M (1996). When is diffuse-field theory applicable? *Applied Acoustics*, 49: 197–207.

Hou Q, Cai M, Wang H (2017). Dynamic modeling of traffic noise in both indoor and outdoor environments by using a ray tracing method. *Building and Environment*, 121: 225–237.

Kang J (1996a). Acoustics in long enclosures with multiple sources. *The Journal of the Acoustical Society of America*, 99: 985–989.

Kang J (1996b). The unsuitability of the classic room acoustical theory in long enclosures. *Architectural Science Review*, 39: 89–94.

Kang J (2000). Sound propagation in street canyons: Comparison between diffusely and geometrically reflecting boundaries. *The Journal of the Acoustical Society of America*, 107: 1394–1404.

Kang J (2001). Sound propagation in interconnected urban streets: A parametric study. *Environment and Planning B: Planning and Design*, 28: 281–294.

Kang J (2002). Acoustics of Long Spaces: Theory and Design Guidance. London: Thomas Telford Publishing.

Kryter KD (1962). Methods for the calculation and use of the articulation index. *The Journal of the Acoustical Society of America*, 34: 1689–1697.

Kuttruff H (2009). Room Acoustics, 5th edn. New York: Spon Press.

Lehmann EA, Johansson AM (2008). Prediction of energy decay in room impulse responses simulated with an image-source model. *The Journal of the Acoustical Society of America*, 124: 269–277.

Lewers TH, Anderson JS (1984). Some acoustical properties of St Paul's Cathedral, London. *Journal of Sound and Vibration*, 92: 285–297.

Picaut J, Simon L, Polack JD (1999). Sound field in long rooms with diffusely reflecting boundaries. *Applied Acoustics*, 56: 217–240.

Summers JE, Torres RR, Shimizu Y (2004). Statistical-acoustics models of energy decay in systems of coupled rooms and their relation to geometrical acoustics. *The Journal of the Acoustical Society of America*, 116: 958–969.

Visentin C, Prodi N, Valeau V, Picaut J (2015). Experimental analysis of the relationship between reverberant acoustic intensity and energy density inside long rooms. *The Journal of the Acoustical Society of America*, 138: 181–192.

Wang C, Ma H, Wu Y, Kang J (2018). Characteristics and prediction of sound level in extra-large spaces. *Applied Acoustics*, 134: 1–7.

Xiang N, Goggans PM, Jasa T, Kleiner M (2005). Evaluation of decay times in coupled spaces: Reliability analysis of Bayeisan decay time estimation. *The Journal of the Acoustical Society of America*, 117: 3707–3715.

Xiang N, Goggans P, Jasa T, Robinson P (2011). Bayesian characterization of multiple-slope sound energy decays in coupled-volume systems. *The Journal of the Acoustical Society of America*, 129: 741–752.